



HAL
open science

Constitutive expression of Cas9 and rapamycin-inducible Cre recombinase facilitates conditional genome editing in *Plasmodium berghei*

Samhita Das, Tanaya Unhale, Carine Marinach, Belsy del Carmen Valeriano Alegria, Camille Roux, H el ene Madry, Badreddine Mohand Oumoussa, Rogerio Amino, Shiroh Iwanaga, Sylvie Briquet, et al.

► To cite this version:

Samhita Das, Tanaya Unhale, Carine Marinach, Belsy del Carmen Valeriano Alegria, Camille Roux, et al.. Constitutive expression of Cas9 and rapamycin-inducible Cre recombinase facilitates conditional genome editing in *Plasmodium berghei*. *Scientific Reports*, 2025, 15 (1), pp.2949. 10.1038/s41598-025-87114-4. hal-04930876

HAL Id: hal-04930876

<https://hal.science/hal-04930876v1>

Submitted on 5 Feb 2025

HAL is a multi-disciplinary open access archive for the deposit and dissemination of scientific research documents, whether they are published or not. The documents may come from teaching and research institutions in France or abroad, or from public or private research centers.

L'archive ouverte pluridisciplinaire **HAL**, est destin ee au d ep ot et  a la diffusion de documents scientifiques de niveau recherche, publi es ou non,  emanant des  tablissements d'enseignement et de recherche fran ais ou  trangers, des laboratoires publics ou priv es.



Distributed under a Creative Commons Attribution 4.0 International License



OPEN Constitutive expression of Cas9 and rapamycin-inducible Cre recombinase facilitates conditional genome editing in *Plasmodium berghei*

Samhita Das¹, Tanaya Unhale¹, Carine Marinach¹, Belsy del Carmen Valeriano Alegria^{1,5}, Camille Roux¹, H el ene Madry², Badreddine Mohand Oumoussa², Rogerio Amino³, Shiroh Iwanaga⁴, Sylvie Briquet^{1,6}✉ & Olivier Silvie^{1,6}✉

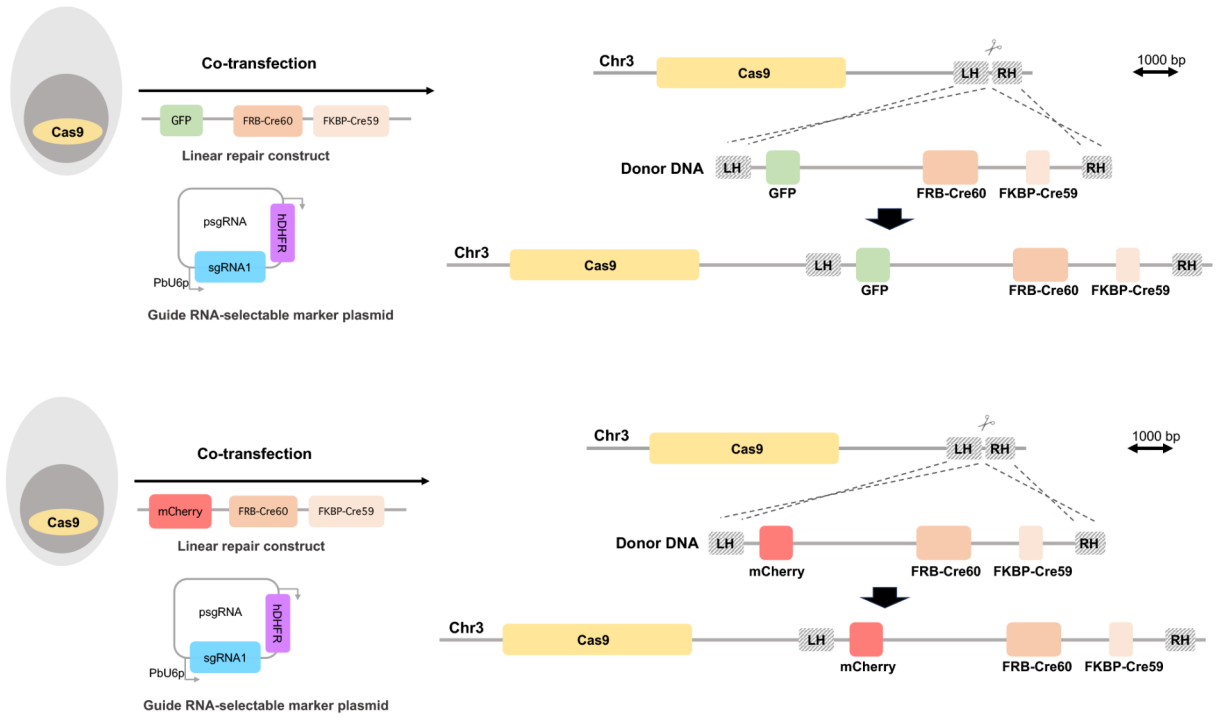
Malaria is caused by protozoan parasites of the genus *Plasmodium* and remains a global health concern. The parasite has a highly adaptable life cycle comprising successive rounds of asexual replication in a vertebrate host and sexual maturation in the mosquito vector *Anopheles*. Genetic manipulation of the parasite has been instrumental for deciphering the function of *Plasmodium* genes. Conventional reverse genetic tools cannot be used to study essential genes of the asexual blood stages, thereby necessitating the development of conditional strategies. Among various such strategies, the rapamycin-inducible dimerisable Cre (DiCre) recombinase system emerged as a powerful approach for conditional editing of essential genes in human-infecting *P. falciparum* and in the rodent malaria model parasite *P. berghei*. We previously generated a DiCre-expressing *P. berghei* line and validated it by conditionally deleting several essential asexual stage genes, revealing their important role also in sporozoites. Another potent tool is the CRISPR/Cas9 technology, which has enabled targeted genome editing with higher accuracy and specificity and greatly advanced genome engineering in *Plasmodium* spp. Here, we developed new *P. berghei* parasite lines by integrating the DiCre cassette and a fluorescent marker in parasites constitutively expressing Cas9. Owing to the dual integration of CRISPR/Cas9 and DiCre, these new lines allow unparalleled levels of gene modification and conditional regulation simultaneously. To illustrate the versatility of this new tool, we conditionally knocked out the essential gene encoding the claudin-like apicomplexan micronemal protein (CLAMP) in *P. berghei* and confirmed the role of CLAMP during invasion of erythrocytes.

Keywords *Plasmodium*, Malaria, CRISPR, Conditional mutagenesis

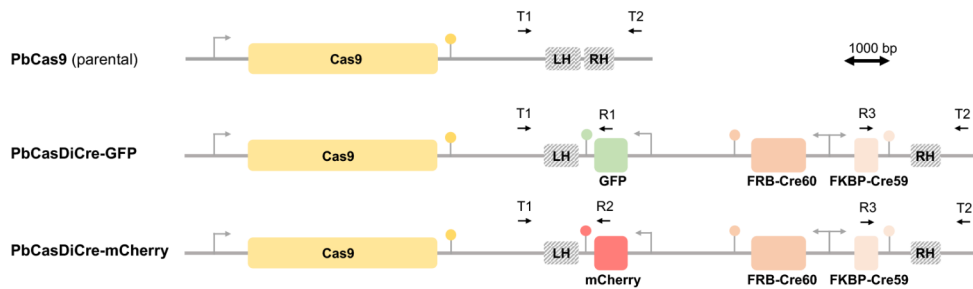
Malaria is a life-threatening disease that is still prevalent in many parts of the world¹. The causative organism, *Plasmodium* spp, is transmitted through the bite of an infected female *Anopheles* mosquito, which releases sporozoites into the mammalian skin. Sporozoites migrate in the skin, enter the blood circulation and travel to the liver. In the liver, sporozoites infect hepatocytes by forming a parasitophorous vacuole (PV) within which they further develop until the release of merozoites into the blood. Merozoites invade erythrocytes, initiating the symptomatic blood stage of infection. A fraction of the blood stage parasites differentiates into gametocytes, which can be taken up by a mosquito during its blood meal. In the mosquito, the parasite forms sporozoites that invade the salivary glands for transmission to a new mammalian host².

¹Sorbonne Universit e, CNRS, Inserm, Centre d'Immunologie et des Maladies Infectieuses, CIMI, F-75013 Paris, France. ²Sorbonne Universit e, Inserm, Production et Analyse des donn ees en Sciences de la vie et Sant e, PASS, Plateforme Post-g enomique de la Piti e-Salp etri re, P3S, F-75005 Paris, France. ³Institut Pasteur, Universit e Paris Cit e, Malaria Infection and Immunity Unit, F-75015 Paris, France. ⁴Research Center for Infectious Disease Control, Department of Molecular Protozoology, Suita, Osaka 565-0871, Japan. ⁵Present address: Institut Pasteur, Laboratory of Ecology and Emergence of Arthropod-borne Pathogens, Paris, France. ⁶Sylvie Briquet and Olivier Silvie contributed equally to this work. ✉email: sylvie.briquet@inserm.fr; olivier.silvie@inserm.fr

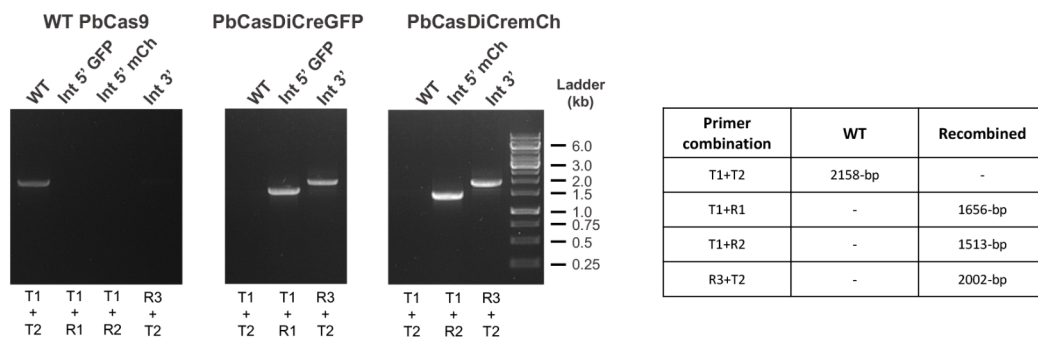
A



B



C



The various stages in the life cycle of *Plasmodium spp* are being studied to identify essential cellular processes, molecular targets and vaccine antigens. *P. berghei* is a widely studied rodent malaria model parasite, owing to the physiological similarities with human malaria and ease in laboratory manipulations. Genome editing tools have significantly improved our knowledge on the role of parasite genes, however, functions of many protein-coding genes are yet to be revealed. Transfection of *Plasmodium* parasites is typically performed in asexual blood stages, precluding loss-of-function mutations of genes that are essential in this part of the life cycle. In recent years, gene manipulation strategies have evolved allowing researchers to conditionally control gene expression³. The dimerisable Cre (DiCre) recombinase system emerged as a powerful tool for conditional gene deletion, first established in *Toxoplasma gondii*⁴ in the Apicomplexan phylum and then adapted in *P. falciparum*^{5,6} and *P. berghei*⁷. The DiCre system functions via expression of the Cre recombinase, split into two separate, inactive polypeptides, each fused to a different rapamycin-binding protein. Rapamycin-induced heterodimerization of

◀ **Fig. 1.** Generation of PbCasDiCre parasites. **(A)** Strategy to integrate DiCre and GFP/mCherry cassettes into Cas9-expressing parasites using CRISPR. The PbCas9 parasites were co-transfected with a linearized DNA repair construct containing the two Cre components and a GFP or mCherry cassette, and with a plasmid encoding a sgRNA guide and a pyrimethamine-resistance cassette (hDHFR). Following Cas9-mediated DNA cleavage, the repair construct was integrated by double crossover recombination at the *p230p* locus downstream of the Cas9 cassette. LH, left homology arm; RH, right homology arm. **(B)** Schematic of the *p230p* locus of parental PbCas9 and transgenic PbCasDiCre-GFP and PbCasDiCre-mCherry parasites. Genotyping primers are indicated by arrows (T, test; R, recombinant). The loci and constructs are drawn at scale in A and B. Scale bar, 1 kb. **(C)** PCR analysis of the genomic DNA obtained from the parental PbCas9 line and the two recombinant lines PbCasDiCre-GFP and PbCasDiCre-mCherry. Confirmation of the expected recombination events was achieved with primer combinations specific for 5' or 3' integration. A wild type-specific PCR reaction (WT) confirmed the absence of residual parental parasites in the PbCasDiCre-GFP and PbCasDiCre-mCherry transgenic lines. The size of the expected amplicons is indicated in the table. The uncropped images of the gels are shown in Supplementary Fig. S3A.

the two components in the presence of rapamycin restores recombinase activity. The active Cre recognises short 34 bp sequences called *lox* sites, allowing excision of the floxed (flanked by *lox*) DNA sequences with very high efficiency. Along with the efficiency of Cre recombinase, the introduction of *lox* sites is key to efficient genome editing. *Lox* sites can be introduced within the ORF as an artificial intron⁵ or within endogenous introns or UTRs. We previously generated a *P. berghei* line expressing the DiCre cassette and illustrated how this tool allows the study of essential genes not only in asexual blood stages, but also in other stages of the parasite life cycle⁷. Conditional gene deletion in PbDiCre parasites revealed the essential role of *ama1*, *ron2*, *ron4* and *clamp* genes in blood stages and sporozoites^{8,9}. In these studies, a two-step strategy was employed to insert *lox* sites upstream and downstream of the target gene.

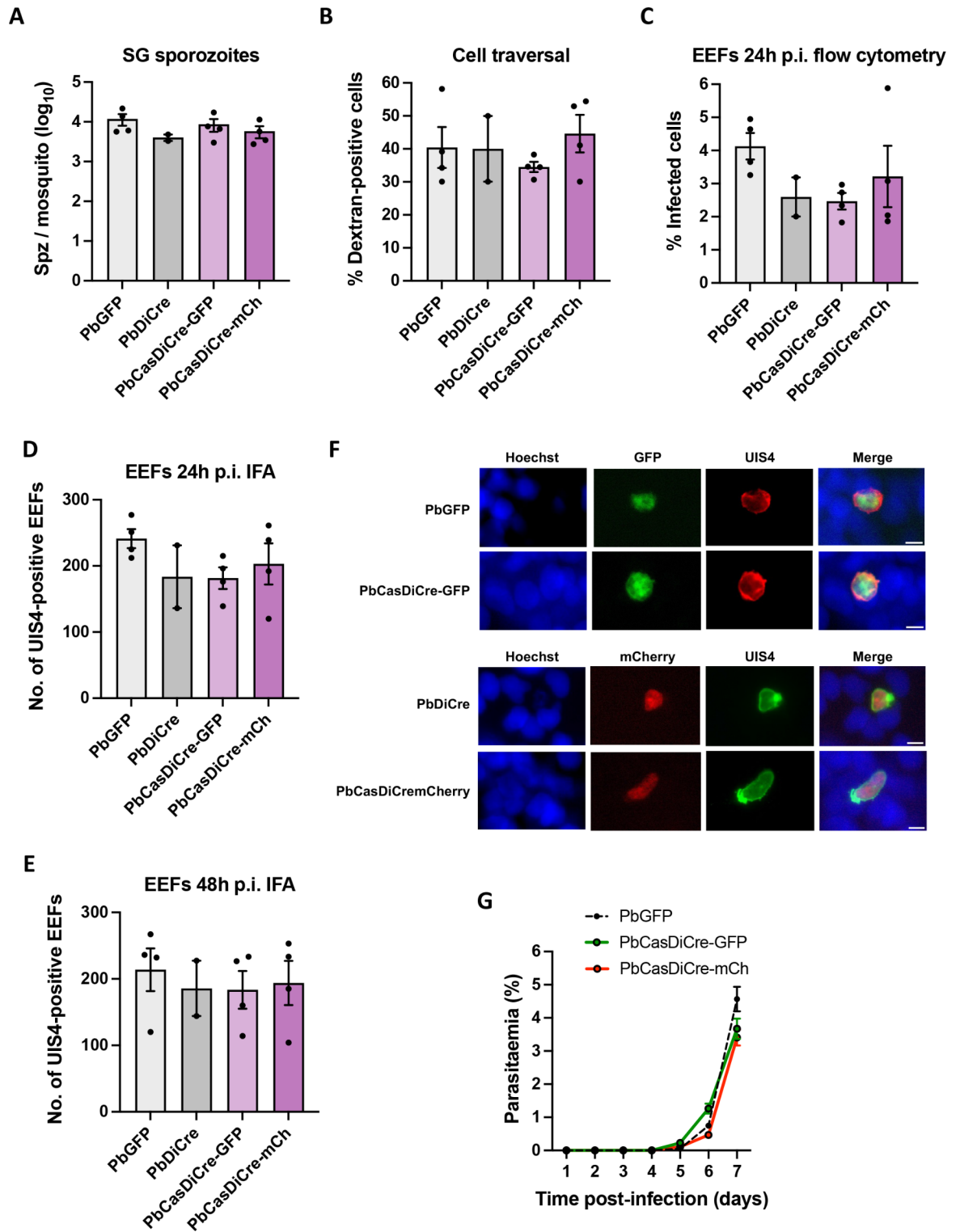
The past decade also observed a novel emergence of versatile clustered regularly interspaced short palindromic repeats (CRISPR)/CRISPR-associated (Cas) nucleases and their variants with increased genome editing efficiency and specificity. The system consists of a Cas9 nuclease which forms a complex with a single-guide RNA (sgRNA) to precisely generate a double-strand break (DSB) in the genome. As *Plasmodium* lacks the classical non-homologous end-joining (NHEJ) pathway, DSB can only be repaired by homology-directed recombination (HDR) with a provided donor DNA template¹⁰. Since its implementation, there has been many technical developments in the use of CRISPR/Cas9 in *Plasmodium spp.* The latest improvements of the CRISPR/Cas9 system in *P. berghei* involve co-transfection of parasites constitutively expressing Cas9 from an integrated cassette with a linearized donor template together with a plasmid encoding one or two sgRNA¹¹. This approach was shown to allow genome editing with very high efficiency, from gene knockout to targeted mutagenesis¹¹.

Here, we aimed to combine both the CRISPR and DiCre strategies and generated *P. berghei* parasite lines harboring Cas9 and DiCre cassettes integrated into their genome together with a fluorescent marker. Our goal was to produce a useful, efficient and versatile tool allowing a wide range of genetic modifications in *P. berghei*, from targeted mutagenesis to conditional genome editing. For this purpose, we used parasites of a *P. berghei* PbCas9 line containing a Cas9 cassette integrated in the dispensable *p230p* locus under the control of the *HSP70* promoter for constitutive expression¹², that was generated similar to the transgenic *P. berghei* line containing the cas9 expression cassette introduced into the *c/d-ssu-rna* gene locus¹¹. Parasites of this line do not contain a drug-selectable marker. We modified the PbCas9 line using CRISPR to further integrate at the same locus a DiCre cassette and a fluorescent marker (either GFP or mCherry) to facilitate parasite detection. We generated two lines and named them *PbCasDiCre-GFP* and *PbCasDiCre-mCherry*, containing the GFP or the mCherry fluorescent marker, respectively. To illustrate the versatility and efficiency of this new tool, we used CRISPR to modify the essential gene *clamp* in one single step, and show that rapamycin-induced conditional deletion of *clamp* impairs merozoite invasion.

Results

Generation of fluorescent transgenic *P. berghei* lines expressing both Cas9 and dimerisable Cre

Constitutive expression of Cas9 allows genome editing in *P. berghei* with high efficiency following transfection of sgRNA and a linear donor template for DNA repair by homologous recombination¹¹. In order to combine the Cas9 and DiCre systems, we used CRISPR to genetically modify PbCas9 parasites that constitutively express Cas9 from a cassette integrated at the dispensable *p230p* gene locus, which were generated similar to the transgenic *P. berghei* line containing the Cas9 expression cassette introduced into the *c/d-ssu-rna* gene locus^{11,12}. A 20-base sgRNA target was selected in the *p230p* locus, downstream of the integrated Cas9 cassette, and the corresponding sequence was cloned downstream of PbU6 promoter into a sgRNA plasmid containing a pyrimethamine-resistance cassette (Fig. 1A). For the repair DNA template, we used the same DiCre cassette as previously described⁷. This cassette consists of the N-terminal Cre 59 (residues Thr19-Asn59) and C-terminal Cre 60 (Asn60-Asp343) portions of the Cre fused at their N-terminus to FKBP12 and FRB, respectively. These two components were placed under control of the constitutive bidirectional promoter eEF1alpha, and followed by the 3' untranslated region (UTR) from PfCAM and PbHSP70, respectively⁷. In this construct, we further incorporated a fluorescent marker (GFP or mCherry, respectively) under the control of the *hsp70* promoter and the 3' UTR of PbDHFR. On each side of the construct, we inserted 5' and 3' homology fragments for integration at the *p230p* locus, downstream of the Cas9 cassette (Fig. 1A). The donor template DNA was assembled in a plasmid and linearized prior to transfection.



Following the transfection of *PbCas9* parasites with the sgRNA plasmid and the linearized donor template DNA, integration of the repair construct by double homologous recombination results in the generation of parasites containing three cassettes integrated at the *p230p* locus: the Cas9, the DiCre and the GFP or mCherry cassettes (Fig. 1B). Transfected parasites were exposed to pyrimethamine to select parasites containing the sgRNA plasmid. Following withdrawal of the selection drug, recombinant parasites were recovered and genotyped by PCR, using primer combinations specific for the parental or the recombined locus, respectively (Fig. 1C). Genotyping PCR confirmed that the selected parasites had integrated the DiCre construct, with no remnant of the parental parasites (Fig. 1C), consistent with very high efficiency achieved with the integrated Cas9 approach¹¹. PCR amplicons were verified by Sanger sequencing. We also conducted a genome-wide sequence analysis using Oxford Nanopore Technology in order to verify the integrity of the DiCre and GFP/mCherry cassettes, and their correct integration at the expected locus. Alignment of the reads from PbCasDiCre-GFP and

◀ **Fig. 2.** Phenotypic characterization of PbCasDiCre parasites. **(A)** Comparison of sporozoite numbers isolated from salivary glands of female mosquitoes infected with the control lines, PbGFP and PbDiCre, or with the new PbCasDiCre-GFP and PbCasDiCre-mCherry transgenic lines. Results shown are mean \pm SEM of two to four independent experiments ($p=0.39$, one-way ANOVA). **(B)** Quantification of traversed (dextran-positive) HepG2 cells by FACS after incubation for 3 h with PbGFP, PbDiCre, PbCasDiCre-GFP or PbCasDiCre-mCherry salivary gland sporozoites in the presence of fluorescent dextran. Results shown are mean \pm SEM of two to four independent experiments ($p=0.60$, one-way ANOVA). **(C)** Quantification of infected (GFP- or mCherry-positive) HepG2 cells by flow cytometry 24 h post-infection with PbGFP, PbDiCre, PbCasDiCre-GFP or PbCasDiCre-mCherry salivary gland sporozoites. Results shown are mean \pm SEM of two to four independent experiments ($p=0.32$, one-way ANOVA). **(D), (E)** Quantification of UIS4-labelled exo-erythrocytic forms (EEFs) in HepG2 cells as determined by fluorescence microscopy 24 h **(D)** and 48 h **(E)** post-infection. Results shown are mean \pm SEM of two to four independent experiments ($p=0.33$ in D, 0.65 in E, one-way ANOVA). **(F)** Images of PbCasDiCre-GFP and PbCasDiCre-mCherry EEFs compared to the controls PbGFP and PbDiCre 48 h p.i. in HepG2 cells. The parasitophorous vacuole membrane was labelled with anti-UIS4 antibodies and nuclei were stained with Hoechst 33342. Scale bar, 5 μ m. **(G)** Parasite development was compared in vivo post-sporozoite injection. C57BL/6J mice ($n=3$) were injected intravenously with 1×10^3 PbGFP, PbCasDiCre-GFP or PbCasDiCre-mCherry sporozoites. Parasitaemia was then followed by flow cytometry. The data shown are mean \pm SEM of 3 mice per group.

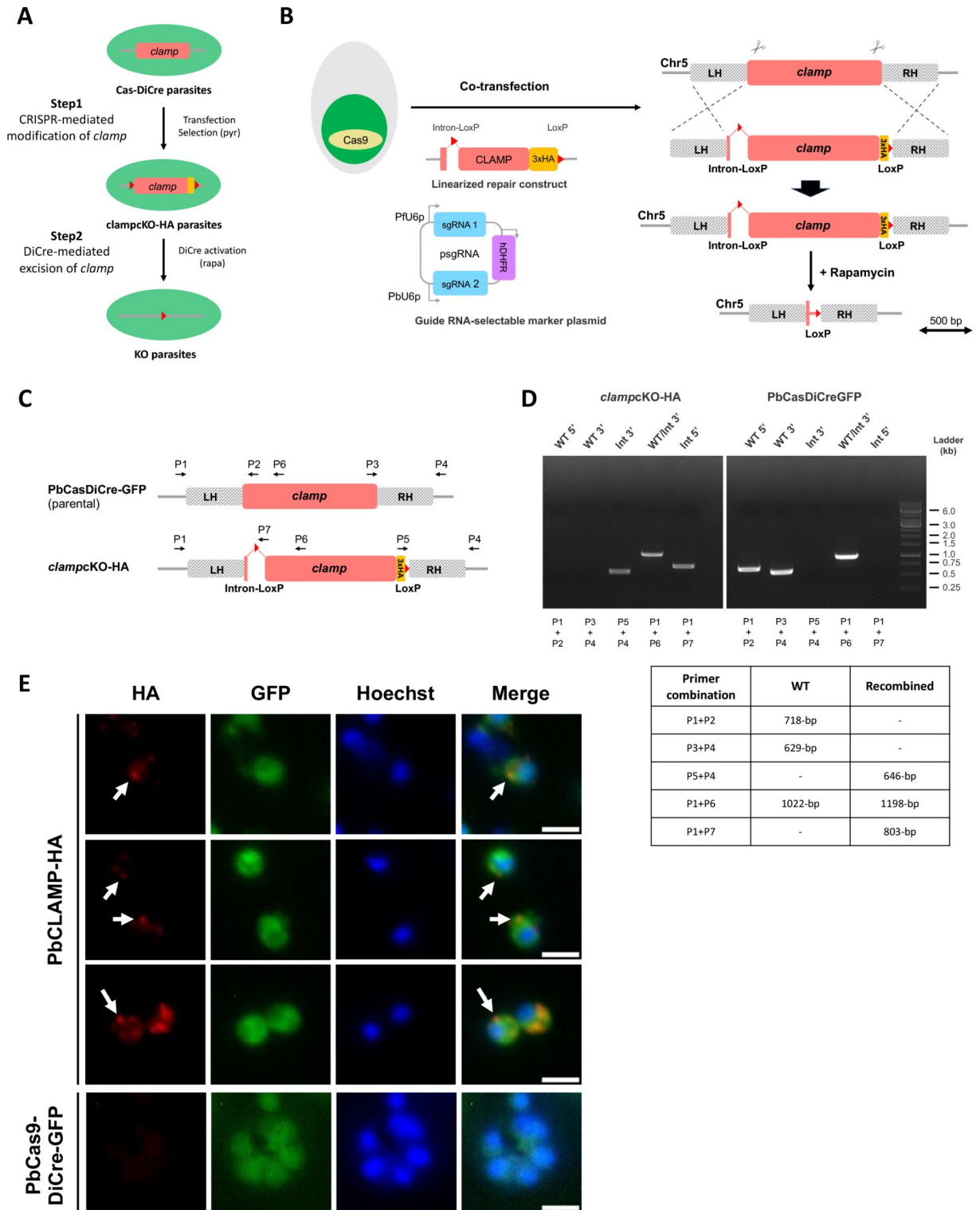
PbCasDiCre-mCherry parasite gDNA to the predicted recombined *p230p* locus showed an average coverage of 47 to 73X encompassing the entire locus, confirming the correct integration of the fluorescent and DiCre cassettes downstream of Cas9, as expected (Supplementary Fig. S1). In contrast, alignment of the reads from parental PbCas9 parasite gDNA to the predicted modified *p230p* locus of PbCasDiCre-GFP and PbCasDiCre-mCherry parasites showed 3 uncovered regions, corresponding to the GFP or mCherry cassette and the two DiCre components, respectively (Supplementary Fig. S1). The recombinant parasite lines were exposed to 5-fluorocytosine (5-FC) to eliminate any residual parasite harboring the sgRNA plasmid, resulting in pure, drug-selectable marker-free PbCasDiCre-GFP and PbCasDiCre-mCherry parasite populations.

Transgenic PbCasDiCre-GFP and PbCasDiCre-mCherry parasites complete their life cycle normally

We examined the progression of the modified parasites through the life cycle, by comparing with lab-standardised control lines to exclude any possible effects of the introduction of the cassettes. Mice were infected with PbCasDiCre-GFP or PbCasDiCre-mCherry parasites and used to feed *A. stephensi* mosquitoes. We then monitored parasite development inside infected mosquitoes using fluorescence microscopy. Both transgenic lines colonized the mosquito midguts to form oocysts, and developed into sporozoites that invaded the mosquito salivary glands. Similar numbers of salivary gland sporozoites were obtained from mosquitoes infected with the modified parasite lines as compared to PbGFP or PbDiCre parasites used as controls (Fig. 2A), showing that PbCasDiCre parasites develop normally inside the vector. To check the development of the mammalian liver stages, PbCasDiCre-GFP and PbCasDiCre-mCherry sporozoites were isolated from the salivary glands of infected mosquitoes and incubated with HepG2 cells. Transgenic sporozoites showed normal cell traversal activity, as determined using a dextran-based cell wound repair assay (Fig. 2B), and formed similar numbers of exo-erythrocytic forms (EEFs) as the control PbGFP and PbDiCre parasites, as determined by flow cytometry 24 h post-infection (Fig. 2C) and by fluorescence microscopy 24 and 48 h post-infection after labelling of the parasitophorous vacuole membrane marker UIS4 (Fig. 2D, E and F). We also checked the infectivity of PbCasDiCre-GFP and PbCasDiCre-mCherry sporozoites in vivo in C57BL/6J mice. After intravenous inoculation of the parasites, mice injected with PbCasDiCre-GFP and PbCasDiCre-mCherry parasites all developed a patent parasitaemia, with similar pre-patency periods and blood-stage growth as control PbGFP parasites (Fig. 2G). Altogether, these data confirm that *P. berghei* parasites constitutively expressing Cas9 and DiCre are capable of completing the parasite life cycle normally, and thus provide a suitable platform to study gene function across the life cycle.

CRISPR-assisted conditional knockout of *clamp* in *P. berghei*

In order to validate the Cas9 and DiCre combination, we used the PbCasDiCre-GFP line to conditionally delete the gene encoding the Claudin-like apicomplexan microneme protein (CLAMP, PBANKA_0514200). CLAMP plays an essential role during invasion by *Toxoplasma gondii* tachyzoites and in *P. falciparum* asexual blood stages^{13,14}. Being essential for blood stage growth, CLAMP is refractory to conventional gene deletion, thereby requiring a conditional genome editing strategy. In a previous study using PbDiCre parasites, we showed that CLAMP is involved during blood stage growth and in gliding motility and infectivity of sporozoites in *P. berghei*⁸. In that study, conditional knockout parasites were obtained after introducing LoxN sites upstream and downstream of *clamp* gene in a two-step strategy requiring two successive transfections⁸. The blood stage growth of CLAMP conditional knockout parasites exposed to rapamycin was reduced as compared to control parasites. Here, in order to allow functional studies in merozoites, we used a different one-step strategy to introduce a first LoxP site inside an artificial intron, as described in *P. falciparum*⁵, and a second LoxP site immediately downstream of the STOP codon (Fig. 3A-B). A triple HA tag was introduced before the STOP codon for C-terminal tagging of CLAMP. Using this strategy, Cre-mediated recombination should result in immediate and complete suppression of CLAMP expression. Two guide RNAs were selected in the *clamp* locus, in the 5' and 3' regions of the coding sequence, respectively, and cloned into a single plasmid containing PbU6 and PFU6 promoters (Fig. 3B)¹¹. We



chose to use two guide RNAs instead of one as it has been shown to increase the recombination rate when recombination sites in the target locus are distant¹¹. The donor DNA template carrying a modified *clamp* gene with an artificial intron taken from the *P. berghei* *slarp* gene (PBANKA_0902100)¹⁵ and containing the first LoxP site, a 3xHA tag and a second LoxP site, was provided as a synthetic gene and linearized before transfection.

Following the transfection of PbCasDiCre-GFP parasites with the double sgRNA plasmid targeting *clamp* and the linearized donor template DNA, integration of the repair construct by double homologous recombination results in the generation of parasites containing a floxed *clamp* gene with a C-terminal 3xHA tag (Fig. 3A, B). Recombinant parasites were selected with pyrimethamine and genotyped by PCR, using primer combinations specific for the parental or the recombined locus, respectively (Fig. 3C, D). Genotyping PCR confirmed that the selected parasites had integrated the repair construct, with no remnant of the parental parasites (Fig. 3D). PCR amplicons were verified by Sanger sequencing. We also conducted a genome wide sequence analysis using

◀ **Fig. 3.** Generation of *clamp*KO-HA parasites. (A) Overview of the strategy used for conditional knockout of *clamp* using CRISPR/Cas9 and DiCre. (B) Strategy to flox the *clamp* gene in PbCasDiCre-GFP using CRISPR. PbCasDiCre-GFP parasites were co-transfected with a linearized DNA repair construct containing a floxed *clamp* gene with a C-terminal 3xHA tag, and with a plasmid encoding two sgRNA guides and a pyrimethamine-resistance cassette (hDHFR). Following Cas9-mediated DNA cleavage, the repair construct was integrated by double crossover recombination at the *clamp* locus, resulting in the generation of the *clamp*KO-HA parasite line. (C) Schematic of the *clamp* locus of parental and transgenic *clamp*KO-HA parasites. Genotyping primers are indicated by arrows. The loci and constructs are drawn at scale in B and C. Scale bar, 0.5 kb. (D) PCR analysis of the genomic DNA obtained from the parental PbCasDiCre-GFP and the recombinant *clamp*KO-HA lines. Confirmation of the expected recombination events was achieved with primer combinations specific for 5' or 3' integration. Wild type-specific PCR reactions (WT 5' and 3') confirmed the absence of residual parental parasites in the *clamp*KO-HA line. The size of the expected amplicons is indicated in the table. The uncropped images of the gels are shown in Supplementary Fig. S3B. (E) Immunofluorescence analysis of *clamp*KO-HA merozoites using anti-HA antibodies revealed a polar and punctate distribution of the protein, with no labelling observed in parental untagged parasites. Scale bar, 2 μ m.

Oxford Nanopore Technology in order to verify the integrity of the modified *clamp* locus in the *clamp*KO-HA line. Reads from the *clamp*KO parasite DNA aligned entirely to the expected modified *clamp*KO locus on chromosome 5, with an average coverage of 77X, while alignment of the reads from parental PbCasDiCre-GFP showed 2 uncovered regions around the *clamp* gene locus, matching the LoxP and 3xHA/LoxP sequences, respectively (Supplementary Fig. S2).

Analysis of *clamp*KO-HA merozoites by immunofluorescence using anti-HA antibodies revealed a punctate distribution of the protein which was often predominant at one pole of the parasite (Fig. 3E), reminiscent of the apical accumulation of the protein previously seen in sporozoites⁸. As a control, no labelling was observed in untagged parasites (Fig. 3E).

We then assessed the effects of rapamycin on *clamp*KO parasites during blood-stage growth. A first group of mice with patent parasitaemia was treated with a single oral dose of rapamycin, while mice in a control group were left untreated. We then monitored the parasitaemia over time by flow cytometry. Remarkably, rapamycin-induced excision of *clamp* reduced parasitaemia to nearly zero in a single cycle (< 24 h), as compared to untreated parasites (Fig. 4A), in agreement with an essential role for CLAMP in asexual blood stages. In order to verify that *clamp* gene excision induced by rapamycin exposure was efficient in depleting CLAMP protein, we exposed *clamp*KO parasites to rapamycin in vitro and analyzed the abundance of CLAMP by Western blot using anti-HA antibodies. While in untreated parasites the protein was detected as a single ~ 40 kDa band, consistent with data obtained previously with sporozoites expressing Flag-tagged CLAMP⁸, CLAMP was no longer detected in merozoites after rapamycin treatment (Fig. 4B). The rapid and dramatic decrease of parasitaemia during the first cycle after exposure to rapamycin suggests that CLAMP-deficient parasites are not able to invade erythrocytes. To directly assess the invasive capacity of CLAMP-deficient merozoites, *clamp*KO merozoites were produced in culture in the presence or absence of rapamycin, and injected intravenously into mice. Following inoculation, untreated merozoites efficiently invaded mouse erythrocytes and established a blood stage infection, as evidenced by flow cytometry (Fig. 4C). In sharp contrast, rapamycin-exposed merozoites failed to invade erythrocytes, as evidenced by the absence of detectable parasitaemia after inoculation into mice (Fig. 4C). These data thus demonstrate that CLAMP is required in *P. berghei* merozoites for invasion of erythrocytes, and illustrate the efficacy of the combined Cas9-DiCre approach to investigate parasite gene function.

Discussion

CRISPR has become a standard method for genetic modification in many organisms, including *Plasmodium* spp and other apicomplexan parasites¹⁶. In the rodent malaria model parasite *P. berghei*, improvement of the CRISPR/Cas9 system has been recently achieved through the constitutive expression of Cas9 and the usage of a linear donor template, allowing robust and highly accurate genome editing¹¹. Following transfection of Cas9-expressing parasites with a sgRNA-encoding plasmid, site specific DSB introduced in the genome by Cas9 result in parasite death, unless DNA is repaired by homologous recombination with the linear donor DNA template provided with the sgRNA plasmid during transfection. A short drug selection step eliminates parasites that have not taken up the sgRNA plasmid. This strategy allows recovering recombinant parasites with very high efficiency, close to 100%. Here we used this strategy to modify by CRISPR the dispensable *p230p* locus in PbCas9 parasites to introduce an additional DiCre cassette in the genome of PbCas9 parasites, together with a fluorescence GFP or mCherry cassette to facilitate parasite monitoring. Following transfection, we recovered pure populations of recombinant parasites expressing the combined cassettes, with no detectable persistence of the parental parasites, illustrating the very high efficiency of the CRISPR approach. We show here that Cas-DiCre parasites progress normally through the life cycle, in both the mosquito and mammalian hosts, confirming that expression of Cas9 and DiCre components has no deleterious effect on the parasite viability and infectivity, as previously observed when each component was integrated independently in the parasite genome^{7,11}. While the combination of Cas9 and DiCre does not change the efficacy of each individual tool, the presence of Cas9 greatly facilitates insertion of Lox sites into the parasite genome for subsequent DiCre-mediated recombination, without the need to integrate any drug-selectable marker in the target locus.

We have previously implemented the DiCre system in *P. berghei* parasites and illustrated how this approach can be used to conditionally delete essential genes before transmission to mosquitoes to investigate gene function in sporozoites^{7–9,17}. This strategy allowed us to demonstrate the role of AMA1 and RONs during invasion of

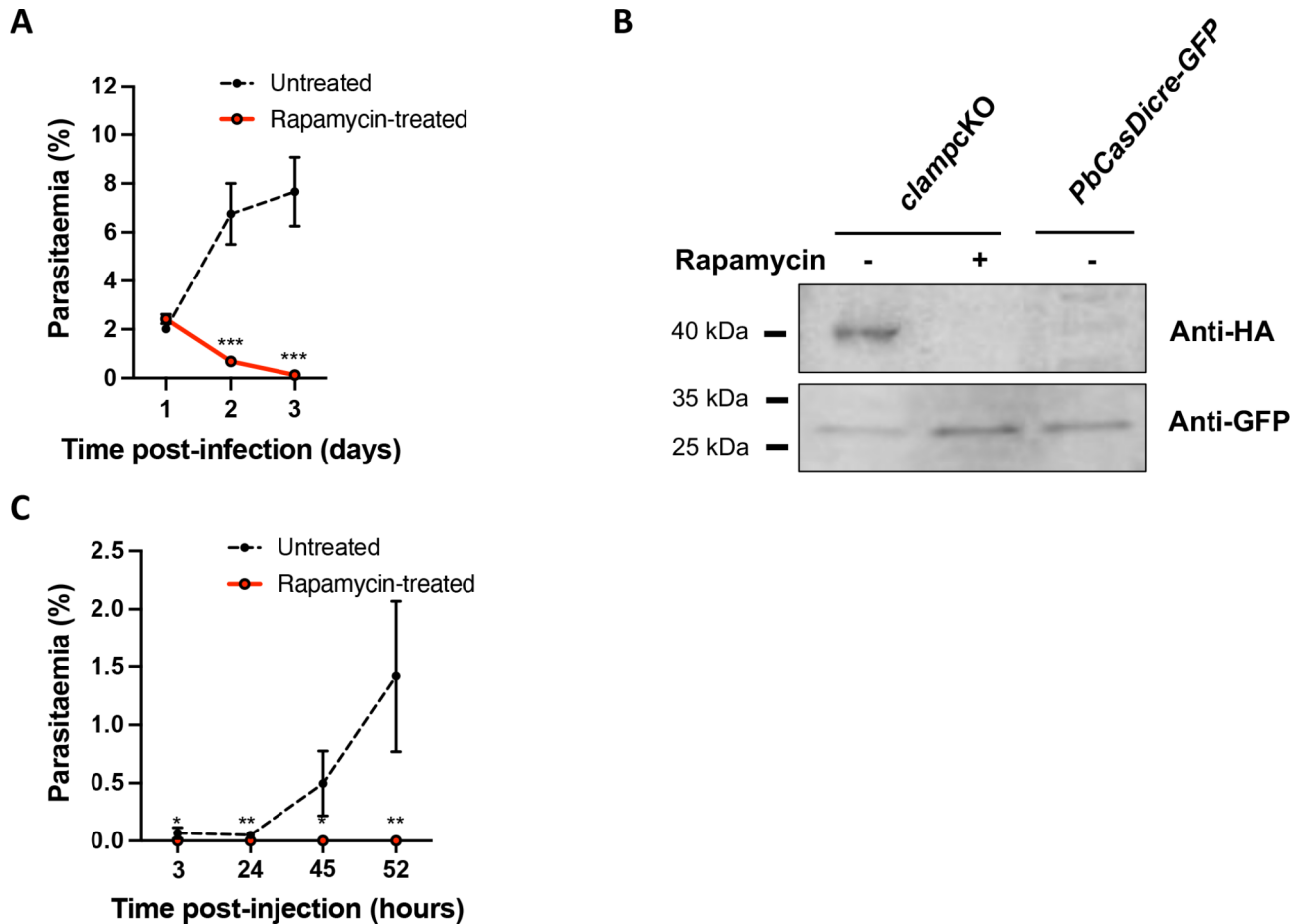


Fig. 4. Conditional knockout of *clamp* abrogates merozoite infectivity. **(A)** Blood stage growth of rapamycin-treated and untreated *clampcKO*-HA parasites. Rapamycin was administered at day 1. The graph shows the parasitaemia (mean \pm SEM) in groups of 5 mice, as quantified by flow cytometry based on GFP detection. ***, $p < 0.001$ (unpaired t-test). **(B)** Western blot analysis of blood stage schizont lysates from untreated or rapamycin-treated *clampcKO*-HA parasites, and control parental PbCasDiCre-GFP parasites, using anti-HA antibodies to detect CLAMP. GFP was used as a loading control. The uncropped images of the blots are shown in Supplementary Fig. S4. **(C)** *clampcKO*-HA parasites were cultured for 18 h in the presence or absence of rapamycin. Merozoites were then purified and injected intravenously into mice. The graph shows the parasitaemia (mean \pm SEM) in groups of 3 mice, as quantified by flow cytometry based on GFP detection. *, $p < 0.05$; **, $p < 0.01$ (unpaired t-test).

mosquito salivary glands and mammalian hepatocytes⁹, as well as the role of CLAMP in sporozoite motility and infectivity⁸. In these studies, Lox sites were inserted upstream and downstream of the target genes in two steps, requiring two successive transfections. Another limitation of the standalone DiCre approach was that a drug resistance cassette had to be integrated for the selection of modified parasites, thus limiting iterative genetic modifications. Here, we used CRISPR to insert two Lox sites in *clamp* gene in one single transfection. A short selection step with pyrimethamine was only used to select for parasites harboring the sgRNA plasmid, and following drug withdrawal we obtained pure populations of drug selectable marker-free *clampcKO* parasites. In addition, one of the Lox sites was inserted inside a synthetic intron, as previously described in *P. falciparum*⁵. The advantage of such a strategy is that rapamycin-induced recombination results in immediate disruption of the expression unit, allowing phenotypic analysis in merozoites.

We have previously shown that CLAMP is required for *P. berghei* blood stage growth⁸. Here, rapamycin-induced disruption of *clamp* did not impair maturation of schizonts and production of merozoites in vitro. However, CLAMP-deficient merozoites were not capable of reinvading erythrocytes in vivo after inoculation into mice. This result demonstrates that CLAMP is required for host cell invasion, as described in *Toxoplasma gondii*^{13,14}. Immunofluorescence assays revealed a punctate distribution of HA-tagged CLAMP in merozoites. Whether CLAMP localizes to specific subsets of micronemes in merozoites and contributes to rhoptry secretion during host cell invasion, as in *T. gondii* tachyzoites^{13,14}, deserves further investigation.

This study illustrates that the combination of Cas9 and DiCre systems provides a robust and versatile platform allowing diverse genome editing strategies in *P. berghei*, including conditional gene disruption to decipher the function of essential genes across the parasite life cycle. New CRISPR-based methods are emerging

in *Plasmodium*, including scalable genetic screens based on Cas9, as recently implemented in *P. falciparum*¹⁸ and *P. berghei*¹⁹. The Cas-DiCre *P. berghei* lines may represent valuable tools for such CRISPR-based genetic screens, enriching our toolbox for functional studies in the malaria parasite.

Materials and methods

Ethics statement

All animal work was conducted in strict accordance with the Directive 2010/63/EU of the European Parliament and Council on the protection of animals used for scientific purposes. Protocols were approved by the Ethics Committee Charles Darwin N°005 (approval #24845-2020032816248463). The study was conducted in accordance with ARRIVE guidelines (<https://arriveguidelines.org>).

Generation of plasmids for transfection

sgRNA guide plasmids. Using the Chop-Chop (<https://chopchop.cbu.uib.no>) and Benchling (<https://www.benchling.com>) programs, one or two 19–20 bp guide RNA sequences were selected upstream of PAM motifs in each of the target genes (*p230p* or *clamp*). Their complementary oligonucleotides were subsequently designed and optimized in the Takara Primer design tool (<https://www.takarabio.com/learning-centers/cloning/primer-design-and-other-tools>). A guanosine nucleotide was added at the 5' end of the forward oligonucleotide for enhancing transcriptional initiation¹¹. Paired oligonucleotides were annealed and cloned into a *BsmBI*- or *BsaI*-digested psgRNA_Pf-Pb U6_2targets plasmid using the In-Fusion HD Cloning Kit (Takara), resulting in the insertion of the guide RNA immediately downstream of Pfu6 or PbU6 promoter, respectively¹¹. This plasmid contains a *hDHFR-yfcu* cassette, for positive selection by pyrimethamine and negative selection by 5-fluorocytosine (5-FC)^{20,21}. The resulting sgRNA guide plasmids were checked by Sanger sequencing prior to transfection.

Donor DNA templates for DNA repair by double homologous recombination. Donor DNA templates for integrating the DiCre and GFP/mCherry cassettes were assembled as plasmids in four steps. First, the entire DiCre cassette, containing the Cre59 and Cre60 fragments under control of the bidirectional eEF1 α promoter and followed by 3' UTR sequences of PfcAM and PbHSP70, respectively, was amplified by PCR using the previously described DiCre construct⁷ as a template, and cloned into a pBluescript backbone between *SalI* and *EcoRI* sites. Then, fragments from *p230p* corresponding to 5' and 3' homology regions were cloned on each side of the DiCre cassette, between *KpnI* and *XhoI* sites or *NotI* and *SacII* sites, respectively. Finally, a fluorescence expression cassette, consisting of either GFP or mCherry under control of *pbhsp70* promoter and the 3' UTR of *pbdhfr*, was amplified by PCR using genomic DNA from either PbGFP or PbDiCre parasites, respectively, and inserted in the construct at the *XhoI* site. All cloning steps were performed using the CloneAmp HiFi PCR premix and the In-Fusion HD Cloning Kit (Takara). The resulting plasmids were verified by Sanger sequencing (Eurofins Genomics) and linearized with *KpnI* and *SacII* before transfection. The donor template to modify *clamp* locus was provided as a synthetic gene, containing a 529-bp 5' upstream fragment immediately upstream of the ATG of *clamp*, serving for 5' homologous recombination, a 31-bp sequence of the ORF, a 170-bp intron from *slarp* gene containing a LoxP site, a 2643-bp fragment corresponding to the rest of the ORF, a triple HA epitope tag, a STOP codon, a second LoxP site, and a 528-bp 3' downstream fragment serving for 3' homologous recombination. The entire synthetic gene was flanked by two *XhoI* sites allowing linearization prior to transfection. All the primer sequences are listed in Supplementary Table S1.

Experimental animals, parasites and cell lines

Female SWISS mice (6–8 weeks old, from Janvier Labs) were used for all blood stage parasite infections. Parasite lines were maintained in mice through intraperitoneal injections of parasite cryostocks and transmitted to *Anopheles stephensi* mosquitoes for experimental purposes. *P. berghei* sporozoites were isolated from infected female *Anopheles* mosquitoes and intravenously injected into C57BL/6J mice (female, 4–6 weeks old, Janvier Labs). A drop of blood from the tail was collected in 1 ml PBS daily and used to monitor the parasitaemia by flow cytometry. For parasite transfection, schizonts were purified from an overnight culture of the parent parasite line PbCas9¹¹ and transfected with a mix of 10 μ g of sgRNA plasmid and 10 μ g of linearized donor template by electroporation using the AMAXA Nucleofector device (program U033), as previously described²², and immediately injected intravenously into the tail vein of SWISS mice. To permit the selection of resistant transgenic parasites, pyrimethamine (35 mg/L) was added to the drinking water and administered to mice, starting one day after transfection and for a total of 4–5 days. Following withdrawal of pyrimethamine, the mice were monitored daily by flow cytometry to detect the reappearance of parasites. To eliminate parasites carrying the sgRNA plasmid, an additional step of negative selection was performed, by exposing infected mice to 5-FC (Meda Pharma) at 1 mg/mL in the drinking water. When parasitaemia reached at least 1%, mice were anaesthetized by exposure to 3.5% isoflurane and euthanized under anaesthesia via terminal blood draw followed by cervical dislocation. Mouse blood was collected for preparation of cryostocks and isolation of parasites for genomic DNA extraction and genotyping.

Anopheles stephensi mosquitoes were reared at 24–26 °C with 80% humidity and permitted to feed on infected mice that were anaesthetized by intraperitoneal injection of ketamine (100 mg/kg) and xylazine (10 mg/kg), using standard methods of mosquito infection as previously described²³. Mice were then euthanized under anaesthesia by cervical dislocation. Post-feeding, *P. berghei*-infected mosquitoes were kept at 21 °C and fed on a 10% sucrose solution. Salivary gland sporozoites were collected from infected mosquitoes between 21 and 28 days post-feeding, by hand dissection and homogenisation of isolated salivary glands in complete DMEM (DMEM supplemented with 10% FCS, 1% Penicillin-Streptomycin and 1% L-Glutamine). Mosquitoes infected with GFP- or mCherry-expressing parasites were sorted under a fluorescence microscope prior to dissection. HepG2 cells (ATCC HB-8065) were cultured in complete DMEM, as previously described²⁴.

Rapamycin treatment

DiCre recombinase-mediated excision of targeted DNA sequences was achieved by administration of a single dose of 200 µg Rapamycin (1 mg/ml stock, Rapamune, Pfizer) to mice by oral gavage, or by culturing infected erythrocytes for 18 h in the presence of 100 nM rapamycin (from 1 mM stock solution in DMSO, Sigma-Aldrich). Control cultures were exposed to DMSO alone (0.01% vol/vol).

Genotyping PCR

Blood collected from infected mice was passed through a CF11 column (Whatman) to deplete leucocytes. The collected RBCs were then centrifuged and lysed with 0.2% saponin (Sigma) to recover parasite material for genomic DNA isolation using a kit (Qiagen DNA Easy Blood and Tissue Kit), according to the manufacturer's instructions. Genomic DNA served as template for PCR, using specific primer combinations designed to detect the wild-type or recombined loci. All PCR reactions were carried out using Recombinant Taq DNA Polymerase (5U/µL from Thermo Scientific) and standard PCR cycling conditions. All the primer sequences are listed in Supplementary Table S1.

Oxford nanopore technology sequencing

DNA sample preparation. Whole blood was collected from two infected mice at 5–10% parasitaemia and depleted from white blood cells by successive passage on a CF11 column (Whatman) and a Plasmodipur filter (R-Biopharm). After centrifugation of the filtered blood at 1500 rpm for 8 min at room temperature, the supernatant was discarded and the RBC pellet was resuspended in 0.2% saponin (Sigma) in PBS. Parasites were then pelleted by centrifugation at 2800 rpm for 8 min at room temperature and lysed for DNA extraction using the genomic DNA Easy Blood and Tissue kit (Qiagen, cat. #69504), according to the manufacturer's instructions. DNA was kept at 4 °C and never frozen. Following DNA purification, the sample volume was brought to 200 µL with the elution buffer and gDNA was extracted twice with 200 µL Phenol/Chloroform/Isoamyl alcohol to eliminate hemozoin contamination. The total aqueous fraction (360 µL) was treated with the same volume of Chloroform and the top aqueous phase was collected after centrifugation at maximal speed for 5 min at 4 °C. gDNA was supplemented with 1 µL glycogen (10 mg/mL) and was precipitated with 1/10 volume of Sodium Acetate 3 M pH 5.5 and 2 volumes of 100% ethanol. After overnight incubation at -20 °C, gDNA was centrifuged at maximal speed for 20 min at 4 °C, washed twice with 75% ethanol and air-dried for 5 min at room temperature.

Nanopore library preparation and sequencing. The quality, quantity and size of gDNAs from each strain were verified by spectrophotometry (Nanodrop), fluorimetry (Qubit) and microelectrophoresis (TapeStation 4151), respectively, and correspond to the recommendations of Oxford Nanopore Technologies. Two pools of 6 libraries were prepared from at least 400 ng of gDNA from each parasite strain using the SQK-NBD114-24 ligation kit following the supplier's protocol. The gDNAs from one PbCas9, two PbCasDiCre-GFP, two PbCasDiCre-mCherry and one *clamp*CKO sample were multiplexed in each pool. The first pool was sequenced on a MinION R10.4.1 flow cell (Cat#FLO-MIN114) for 30 h, then the flow cell was washed with the kit (WSH004) following the manufacturer's protocol and the second pool was sequenced for 66 h on the same flow cell. Fast5 raw data was generated using ONT's MinKnow v 23.04.5 software and demultiplexing was performed in real time using guppy software (version 6.5.7).

Preparation of reference genomes. The fasta files used as reference genome for read alignment for the PbCas9, PbCasDiCre-GFP, PbCasDiCre-mCherry strains were generated by inserting the sequence of the Cas9, DiCre-GFP and DiCre-mCherry cassettes, respectively, in place of the sequence between bases 196,621 to 213,484 of chromosome 3 of the genome of *P. berghei* strain ANKA "PlasmoDB-64_PbergheiANKA_Genome" from the PlasmoDB database. The reference genome of the *clamp*CKO strain was generated from the fasta file of the PbCasDiCre-GFP strain by inserting the floxed *clamp* cassette into chromosome 5 in place of the sequence between bases 534,064 and 544,607.

Fastq analysis. Fastq files were generated in Super Accuracy (SupAC) mode from Fast5 files using the dorado basecaller (v7.3.11) of the MinKnow software (v24.02.19). Fastq files were analyzed on the Galaxy Nanopore Europe server with the tools Porechop (v0.2.4) for read trimming and map with minimap2 (v2.28) for alignments. Reads from PbCas9 (parental), PbCasDiCre-GFP and PbCasDiCre-mCherry DNA were aligned to the PbCasDiCre-GFP or PbCasDiCre-mCherry reference genomes, respectively. Reads from the PbCasDiCre-GFP (parental) and *clamp*CKO DNA were aligned on the reference *clamp*CKO genome. Alignment files were merged with the Merge BAM Files tool (v1.2.0) for each strain. Coverage was visualized in igv (v2.16.1).

In vitro infections

HepG2 cells were seeded in collagen-coated culture plates, at a density of 30,000 cells/well in a 96-well plate for flow cytometry analysis and immunofluorescence assays, 24 h prior to infection with sporozoites. On the day of infection, the culture medium in the wells was refreshed with complete DMEM, followed by the addition of 10,000 sporozoites/well for flow cytometry analysis or 1,000 sporozoites/well for immunofluorescence assays. Infected cultures were incubated for 3 h at 37 °C. The wells were then washed twice with complete DMEM and then incubated for another 24–48 h at 37 °C before analysis by flow cytometry or fixation for immunofluorescence. For quantification of infected cells by flow cytometry, the cultures were trypsinized after two washes with PBS, followed by addition of complete DMEM and one round of centrifugation. After discarding the supernatant, the cells were directly resuspended in FACS buffer (PBS + 1% FCS) and analyzed on a Guava EasyCyte 6/2L bench cytometer equipped with 488 nm and 532 nm lasers (Millipore). Cell traversal activity was monitored by flow cytometry using a membrane wound-repair assay based on uptake of fluorescent dextran²⁵. For this purpose, HepG2 cells were incubated for 3 h at 37 °C with PbCasDiCre-GFP or PbCasDiCre-mCherry sporozoites in the presence of 1 mg/mL rhodamine- or FITC-conjugated dextran, respectively, before analysis by flow cytometry.

Immunofluorescence assays

For immunofluorescence assays on HepG2 infected cultures, the cells were washed twice with PBS, then fixed with 4% PFA for 10 min followed by two washes with PBS, quenching with 0.1 M glycine for 5 min, permeabilization with 1% Triton X-100 for 5 min before washes with PBS and blocking in PBS with 3% bovine serum albumin (BSA). Cells were then incubated for 1 h with goat anti-UIS4 primary antibody (1:500, Sicgen), followed by Alexa Fluor 594- or Alexa Fluor 488-conjugated donkey anti-goat secondary antibodies (1:1000, Life Technologies). Nuclei were stained with Hoechst 33342 (Life Technologies). Samples were then imaged on a Zeiss Axio Observer.Z1 fluorescence microscope equipped with a LD Plan-Neofluar 40x/0.6 Corr Ph2 M27 objective. The same exposure conditions were maintained for all the conditions in order to allow comparisons. Images were processed with ImageJ for adjustment of contrast. For immunofluorescence on infected erythrocytes, cultures of *clampcKO-HA* and parental (PbCasDiCre-GFP) schizonts were fixed in 4% PFA as described above and permeabilized with Triton X-100. The HA tag was revealed using a rat monoclonal antibody (3F10, Roche) and Alexa Fluor 594-conjugated goat anti-rat secondary antibodies (1:1000, Life Technologies).

Western blot

Mouse blood infected with *clampcKO-HA* parasites (or PbCasDiCre-GFP as a negative control) was cultured overnight in the presence or absence of rapamycin, collected and resuspended in 1X PBS. Parasite pellets were then isolated by centrifugation, resuspended in Laemmli buffer and analyzed by SDS-PAGE under non-reducing conditions. Western blotting was performed using a rat monoclonal antibody against HA (Roche, 3F10) or a control goat polyclonal antibody against GFP (Sicgen, AB0066-20), followed by secondary antibodies coupled with Alexa Fluor 680 or 800 against rat or goat, respectively. Membranes were then analyzed using the InfraRed Odyssey system (Licor).

Statistical analysis

Statistical significance was assessed by one-way or two-way ANOVA or unpaired t tests, as indicated in the figure legends and Supplementary Tables S2–S5. All statistical tests were computed with GraphPad Prism 10 (GraphPad Software). In vitro experiments were performed with a minimum of three technical replicates per experiment. Quantitative source data are provided in Supplementary Tables S2–S5.

Data availability

Sequence data have been deposited in the NCBI's Sequence Read Archive (<https://www.ncbi.nlm.nih.gov/sra/?term=PRJNA1182486>) with the primary accession code PRJNA1182486. Any other data is provided within the manuscript or supplementary information file.

Received: 15 October 2024; Accepted: 16 January 2025

Published online: 23 January 2025

References

- World Malaria Report. 2024; 1–283. (2023).
- Loubens, M. et al. Plasmodium sporozoites on the move: Switching from cell traversal to productive invasion of hepatocytes. *Mol. Microbiol.* **115**, 870–881. <https://doi.org/10.1111/mmi.14645> (2021).
- Briquet, S., Gissot, M. & Silvie, O. A toolbox for conditional control of gene expression in apicomplexan parasites. *Mol. Microbiol.* **117**, 618–631. <https://doi.org/10.1111/mmi.14821> (2022).
- Andenmatten, N. et al. Conditional genome engineering in *Toxoplasma gondii* uncovers alternative invasion mechanisms. *Nat. Methods* **10**, 125–127. <https://doi.org/10.1038/nmeth.2301> (2012).
- Jones, M. L. et al. A versatile strategy for rapid conditional genome engineering using loxP sites in a small synthetic intron in Plasmodium falciparum. *Sci. Rep.* **6** <https://doi.org/10.1038/srep21800> (2016).
- Collins, C. R. et al. Robust inducible cre recombinase activity in the human malaria parasite *Plasmodium falciparum* enables efficient gene deletion within a single asexual erythrocytic growth cycle. *Mol. Microbiol.* **88**, 687–701. <https://doi.org/10.1111/mmi.12206> (2013).
- Fernandes, P. et al. The dimerisable cre recombinase allows conditional genome editing in the mosquito stages of Plasmodium berghei. *PLoS One* **15**. <https://doi.org/10.1371/journal.pone.0236616> (2020).
- Loubens, M. et al. The claudin-like apicomplexan microneme protein is required for gliding motility and infectivity of Plasmodium sporozoites. *PLoS Pathog.* **19**, e1011261. <https://doi.org/10.1371/journal.ppat.1011261> (2023).
- Fernandes, P. et al. The AMA1-RON complex drives Plasmodium sporozoite invasion in the mosquito and mammalian hosts. *PLoS Pathog.* **18**, e1010643. <https://doi.org/10.1371/journal.ppat.1010643> (2022).
- Ghorbal, M. et al. Genome editing in the human malaria parasite Plasmodium falciparum using the CRISPR-Cas9 system. *Nat. Biotechnol.* **32**, 819–821. <https://doi.org/10.1038/nbt.2925> (2014).
- Shinzawa, N. et al. Improvement of CRISPR/Cas9 system by transfecting Cas9-expressing Plasmodium berghei with linear donor template. *Commun. Biol.* **3**. <https://doi.org/10.1038/s42003-020-01138-2> (2020).
- Nishi, T., Kaneko, I., Iwanaga, S. & Yuda, M. PbAP2-FG2 and PbAP2R-2 function together as a transcriptional repressor complex essential for Plasmodium female development. *PLoS Pathog.* **19**. <https://doi.org/10.1371/journal.ppat.1010890> (2023).
- Valleau, D. et al. A conserved complex of microneme proteins mediates rhostry discharge in Toxoplasma. *EMBO J.* **42**. <https://doi.org/10.15252/EMBJ.2022113155> (2023).
- Sidik, S. M. et al. A genome-wide CRISPR screen in Toxoplasma identifies essential apicomplexan genes. *Cell* **166**, 1423–1435. <https://doi.org/10.1016/j.cell.2016.08.019> (2016).
- Silvie, O., Goetz, K. & Matuschewski, K. A sporozoite asparagine-rich protein controls initiation of Plasmodium liver stage development. *PLoS Pathog.* **4**, e1000086. <https://doi.org/10.1371/journal.ppat.1000086> (2008).
- Lee, M. C. S., Lindner, S. E., Lopez-Rubio, J. J. & Llinás, M. Cutting back malaria: CRISPR/Cas9 genome editing of Plasmodium. *Brief. Funct. Genomics* **18**, 281–289. <https://doi.org/10.1093/BFGP/ELZ012> (2019).
- Fernandes, P., Loubens, M., Silvie, O. & Briquet, S. Conditional gene deletion in mammalian and mosquito stages of Plasmodium berghei using dimerizable cre recombinase. *Methods Mol. Biol.* https://doi.org/10.1007/978-1-0716-1681-9_7 (2021).
- Ramaprasad, A. & Blackman, M. J. A scaleable inducible knockout system for studying essential gene function in the malaria parasite. *bioRxiv*. <https://doi.org/10.1101/2024.01.14.575607> (2024).

19. Jonsdottir, T. K. et al. A scalable CRISPR-Cas9 gene editing system facilitates CRISPR screens in the malaria parasite *Plasmodium berghei*. bioRxiv. <https://doi.org/10.1101/2024.04.20.590404> (2024).
20. Braks, J. A. M., Franke-Fayard, B., Kroeze, H., Janse, C. J. & Waters, A. P. Development and application of a positive-negative selectable marker system for use in reverse genetics in Plasmodium. *Nucleic Acids Res.* **34**. <https://doi.org/10.1093/NAR/GNJ033> (2006).
21. Manzoni, G., Briquet, S. & Risco-Castillo, V. A rapid and robust selection procedure for generating drug-selectable marker-free recombinant malaria parasites. *Sci. Rep.* **99210**, 1–10. <https://doi.org/10.1038/srep04760> (2014).
22. Janse, C. J., Ramesar, J. & Waters, A. P. High-efficiency transfection and drug selection of genetically transformed blood stages of the rodent malaria parasite *Plasmodium berghei*. *Nat. Protoc.* **1**, 346–356 (2006).
23. Ramakrishnan, C. et al. Laboratory maintenance of rodent malaria parasites. *Methods Mol. Biol.* **923**, 51–72. https://doi.org/10.1007/978-1-62703-026-7_5 (2013).
24. Silvie, O., Franetich, J. E., Boucheix, C., Rubinstein, E. & Mazier, D. Alternative invasion pathways for plasmodium berghei sporozoites. *Int. J. Parasitol.* **37**, 173–182. <https://doi.org/10.1016/j.ijpara.2006.10.005> (2007).
25. Prudêncio, M., Rodrigues, C. D., Ataíde, R. & Mota, M. M. Dissecting in vitro host cell infection by *Plasmodium sporozoites* using flow cytometry. *Cell. Microbiol.* **10**, 218–224. <https://doi.org/10.1111/j.1462-5822.2007.01032.x> (2008).

Acknowledgements

We thank Jean-François Franetich and Thierry Houpert for rearing of mosquitoes. This work was funded by grants from the Laboratoire d'Excellence ParaFrap (ANR-11-LABX-0024), the Agence Nationale de la Recherche (ANR-20-CE18-0013) and the Fondation pour la Recherche Médicale (EQU201903007823). This work benefited from equipment and services from the P3S core facility, a platform supported by the Conseil Régional d'Ile-de-France, Sorbonne Université, the National Institute for Health and Medical Research (Inserm) and the Biology, Health and Agronomy Infrastructure (IBISA).

Author contributions

S.D. designed and performed experiments, analyzed the data, wrote the main manuscript text and prepared the figures; T.U. performed experiments and analyzed the data; C.M. performed experiments and analyzed the data, and edited the manuscript; B.C.V.A. and C.R. performed experiments; H.M. and B.M.O. performed the sequencing experiments and analyzed the data; R.A. and S.I. provided resources and analyzed the data; S.B. designed and performed experiments and analyzed the data; O.S. analyzed the data, wrote the main manuscript text and prepared the figures. All authors reviewed the manuscript.

Declarations

Competing interests

The authors declare no competing interests.

Additional information

Supplementary Information The online version contains supplementary material available at <https://doi.org/10.1038/s41598-025-87114-4>.

Correspondence and requests for materials should be addressed to S.B. or O.S.

Reprints and permissions information is available at www.nature.com/reprints.

Publisher's note Springer Nature remains neutral with regard to jurisdictional claims in published maps and institutional affiliations.

Open Access This article is licensed under a Creative Commons Attribution 4.0 International License, which permits use, sharing, adaptation, distribution and reproduction in any medium or format, as long as you give appropriate credit to the original author(s) and the source, provide a link to the Creative Commons licence, and indicate if changes were made. The images or other third party material in this article are included in the article's Creative Commons licence, unless indicated otherwise in a credit line to the material. If material is not included in the article's Creative Commons licence and your intended use is not permitted by statutory regulation or exceeds the permitted use, you will need to obtain permission directly from the copyright holder. To view a copy of this licence, visit <http://creativecommons.org/licenses/by/4.0/>.

© The Author(s) 2025